

## Properties of the Convection Scheme in NCEP's Eta Model that Affect Forecast Sounding Interpretation

MICHAEL E. BALDWIN<sup>\*,+</sup> AND JOHN S. KAIN<sup>+</sup>

*Cooperative Institute for Mesoscale Meteorological Studies, University of Oklahoma, Norman, Oklahoma*

MICHAEL P. KAY

*Forecast Systems Laboratory, Boulder, Colorado*

(Manuscript received 19 February 2002, in final form 24 May 2002)

### ABSTRACT

The impact of parameterized convection on Eta Model forecast soundings is examined. The Betts–Miller–Janjić parameterization used in the National Centers for Environmental Prediction Eta Model introduces characteristic profiles of temperature and moisture in model soundings. These specified profiles can provide misleading representations of various vertical structures and can strongly affect model predictions of parameters that are used to forecast deep convection, such as convective available potential energy and convective inhibition. The specific procedures and tendencies of this parameterization are discussed, and guidelines for interpreting Eta Model soundings are presented.

### 1. Introduction

Convective parameterization is a necessary component of mesoscale and larger-scale models. An important function of convective schemes is to generate precipitation in unstable model environments *before* saturation occurs at individual grid points. This helps models to predict the timing of convective initiation more accurately, an obvious benefit for forecasters. However, generation of precipitation is not the most important role of parameterized convection. The more significant function is to modify convective instability and to redistribute moisture in model soundings. By stabilizing vertical columns before saturation occurs over a deep layer, convective parameterizations act to prevent potentially explosive and unrealistic growth of small-scale disturbances, also known as numerical point storms (Lilly 1960; Rosenthal 1979; Molinari and Dudek 1986; Giorgi 1991). A properly formulated convective parameterization can suppress these unrealistic features and can

play an important role in generating accurate quantitative precipitation forecasts (QPF).

The operational convective parameterization in the National Centers for Environmental Prediction Eta Model (Black 1994) is the Betts–Miller–Janjić scheme (Betts 1986; Betts and Miller 1986; Janjić 1994; hereinafter BMJ). Verification of QPF from this model has been favorable ever since it was introduced (Mesinger 1996), and the BMJ scheme is a key factor in this level of performance, particularly for warm-season forecasts. However, certain aspects of this scheme, although designed to produce the best possible QPF, may generate artificial structures in vertical profiles of temperature and humidity, that is, model forecast soundings (Manikin et al. 2000).

This characteristic can be problematic when these soundings are used to forecast certain elements of the weather. For example, forecasters frequently examine model soundings to evaluate the potential for convective activity. Forecast soundings from the Eta Model are useful for predicting convection, but the BMJ scheme can mask important details of the vertical structure and can affect calculations of convective inhibition (CIN), convective available potential energy (CAPE), and other parameters used in the forecast preparation process (Hart et al. 1998). The utility of the soundings could be enhanced considerably if forecasters learned to recognize when the convective scheme has been active in the model and how it has modified thermodynamic profiles.

---

\* Additional affiliation: NOAA/Storm Prediction Center, Norman, Oklahoma.

+ Additional affiliation: NOAA/National Severe Storms Laboratory, Norman, Oklahoma.

---

*Corresponding author address:* Michael E. Baldwin, CIMMS, 1313 Halley Circle, Norman, OK 73069.  
E-mail: mike.baldwin@noaa.gov

Given the important role that model soundings have come to play in the forecast preparation process and the enduring prominence of the Eta Model, a detailed examination of the characteristic structures associated with the BMJ scheme is warranted. These structures are distinctive, and the trained eye can often readily recognize the “signature” of BMJ activity. The purpose of this paper is to provide guidance for forecasters in recognizing the characteristic impact of the BMJ scheme on model soundings, providing a set of skills that will allow them to make more-insightful judgments about model predictions.

We begin by briefly describing how the BMJ scheme operates. This description is followed by a discussion of the effect of the scheme on model soundings, followed by specific examples of the role played by the BMJ scheme. A final summary and discussion concludes the paper.

## 2. Overview of the BMJ scheme

The BMJ parameterization is a convective adjustment scheme, meaning that it determines “reference” profiles of temperature and dewpoint toward which it nudges the model soundings at individual grid points. The first step in the scheme is to locate the most unstable (highest equivalent potential temperature  $\theta_e$ ) model parcel within approximately the lowest 200 hPa above the ground. It “lifts” this parcel to its lifting condensation level (LCL), which it defines as cloud base. From there, the parcel is lifted moist adiabatically until the equilibrium level (EL) is reached. Cloud top is then defined as the highest model level at which the parcel is still buoyant, typically just below the EL. If the parcel is not buoyant at any level, convection is not activated, and the scheme moves on to the next grid column. If the “cloud” is less than 200 hPa deep, the scheme attempts to initiate shallow (nonprecipitating) convection. Otherwise, it checks to see if deep (precipitating) convection can be activated. As will be shown below, the scheme often reverts to shallow convection even when initial estimates of cloud depth are greater than 200 hPa.

### a. Deep convection

Figure 1 shows a sounding in which the most unstable air is found in the first model layer above ground. Cloud base is near 900 hPa, and cloud top is around 200 hPa. Because cloud depth is greater than 200 hPa, the scheme evaluates the potential for deep convection. It generates preliminary convective adjustment, or reference profiles for temperature ( $T_{\text{ref}}$ ) and water vapor ( $q_{\text{ref}}$ ). These profiles are based on mean structures observed around the globe in the wake of deep convection [for additional justification and explanation, see Betts (1986)]. In the scheme,  $T_{\text{ref}}$  is generated first. This curve is anchored at the temperature of the input sounding at cloud base (not the temperature of the moist adiabat at the LCL).

Above cloud base, the lapse rate of  $T_{\text{ref}}$  is based on the previously determined moist adiabat. That is,  $T_{\text{ref}}$  is specified to diverge slowly from the moist adiabat (i.e., have a higher lapse rate) between cloud base and the freezing level and then to converge to the moist adiabat at cloud top (Fig. 1). Specified in this way,  $T_{\text{ref}}$  is slightly unstable.

Once  $T_{\text{ref}}$  is determined,  $q_{\text{ref}}$  is computed using a specified subsaturation profile (Fig. 1). This subsaturation varies depending on the amount of precipitation, entropy increase from convection, and mean cloud temperature (see Janjić 1994). In a rough sense, the higher the precipitation rate and the smaller the increase in entropy, the closer to saturation  $q_{\text{ref}}$  is specified to be. The actual subsaturation variable is the deficit saturation pressure, which is the pressure depth that a parcel must be lifted to reach its LCL (Betts 1982). In more familiar terms, the subsaturation profile can be thought of as profile of dewpoint depression. Typical values for specified dewpoint depression vary linearly (as a function of pressure) from 3°–5°C at cloud base, to 7°–9°C at the freezing level, back to 3°–5°C at cloud top.

Once these preliminary  $T_{\text{ref}}$  and  $q_{\text{ref}}$  profiles are computed, they are compared with the model profiles of temperature  $T$  and water vapor  $q$  to determine if enthalpy ( $C_p T + L_v q$ , where  $C_p$  is the heat capacity of air at constant pressure and  $L_v$  is the latent heat of vaporization) would be conserved if the model sounding were adjusted to the reference profiles. In practical terms, conservation of enthalpy means that latent heat release associated with convection must be accompanied by (and directly proportional to) removal of water vapor from the sounding, that is,

$$\int_{p_b}^{p_t} C_p \Delta T dp = - \int_{p_b}^{p_t} L_v \Delta q dp, \quad (1)$$

where  $\Delta T = (T_{\text{ref}} - T)$ ,  $\Delta q = (q_{\text{ref}} - q)$ , and  $p_b$  and  $p_t$  are the pressure levels at cloud base and cloud top, respectively. For the preliminary  $T_{\text{ref}}$  and  $q_{\text{ref}}$  profiles that the scheme generates (Fig. 1), both temperature ( $C_p \Delta T$ ) and moisture ( $L_v \Delta q$ ) adjustments are positive throughout most of the cloud layer, rather than offsetting (Fig. 2). So, Eq. (1) is not satisfied (a net increase in enthalpy would be realized if the sounding conformed to these profiles).

Because the enthalpy in the cloud layer would not be conserved (which is typically the case for the “first-guess” reference profiles), the reference profiles are adjusted within the scheme until conservation is achieved. That is, with the subsaturation held constant, both  $T_{\text{ref}}$  and  $q_{\text{ref}}$  (at all levels except cloud top) are shifted to the right or left (on a thermodynamic diagram such as a skew  $T$ - $\log p$  diagram) until Eq. (1) is satisfied. In this case, conservation can be achieved by shifting the reference profiles to the left by a few degrees (Fig. 3). With this adjustment to  $T_{\text{ref}}$  and  $q_{\text{ref}}$ , moisture changes are strongly negative (drying) in the lower troposphere

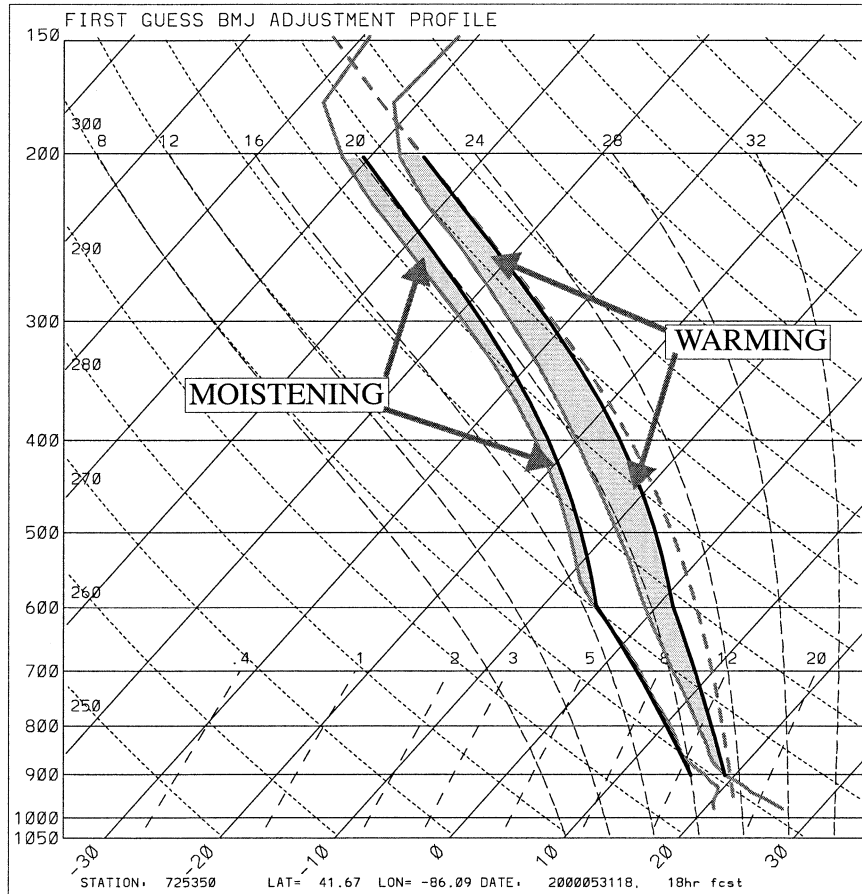


FIG. 1. Model forecast sounding (thick, light solid lines) and preliminary (first guess) BMJ reference profiles (thick, dark solid lines) for an 18-h Eta Model forecast, valid 1800 UTC 31 May 2000 at South Bend, IN (KSBN). Thick, light dashed line indicates the reference moist adiabat determined by the BMJ scheme. Shading highlights the differences in temperature and moisture between the forecast sounding and the preliminary reference profiles.

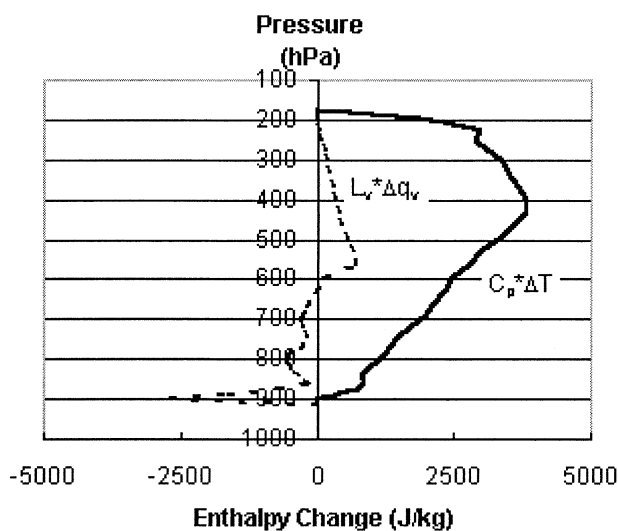


FIG. 2. Vertical profiles of enthalpy change ( $\text{J kg}^{-1}$ ) from temperature (solid line) and water vapor (dashed line) for the preliminary reference profiles shown in Fig. 1.

while temperature changes are mostly positive (warming), peaking in the middle and upper troposphere (Fig. 4). Integrated over the depth of the sounding, the enthalpy changes associated with each of these effects balance exactly, so the net enthalpy change is zero. Moreover, net heating and drying of the column are physically consistent with condensation, latent heat release, and the generation of precipitation, so the BMJ scheme would activate deep convection with this sounding. It is necessary for all of these quantities to be consistent because each grid column is treated as an isolated system when the scheme is called; that is, surrounding grid locations do not factor into the calculations. Within the scheme, net heating can only come from net condensation. Although the condensate could, in principle, be transferred to resolved scales as cloud water, in practice it is all accumulated at the surface as precipitation. It can be shown that the accumulated precipitation is directly proportional to each of the terms in Eq. (1).

Of course, Eq. (1) could also be satisfied if the integral on the left-hand side were negative and the integral on

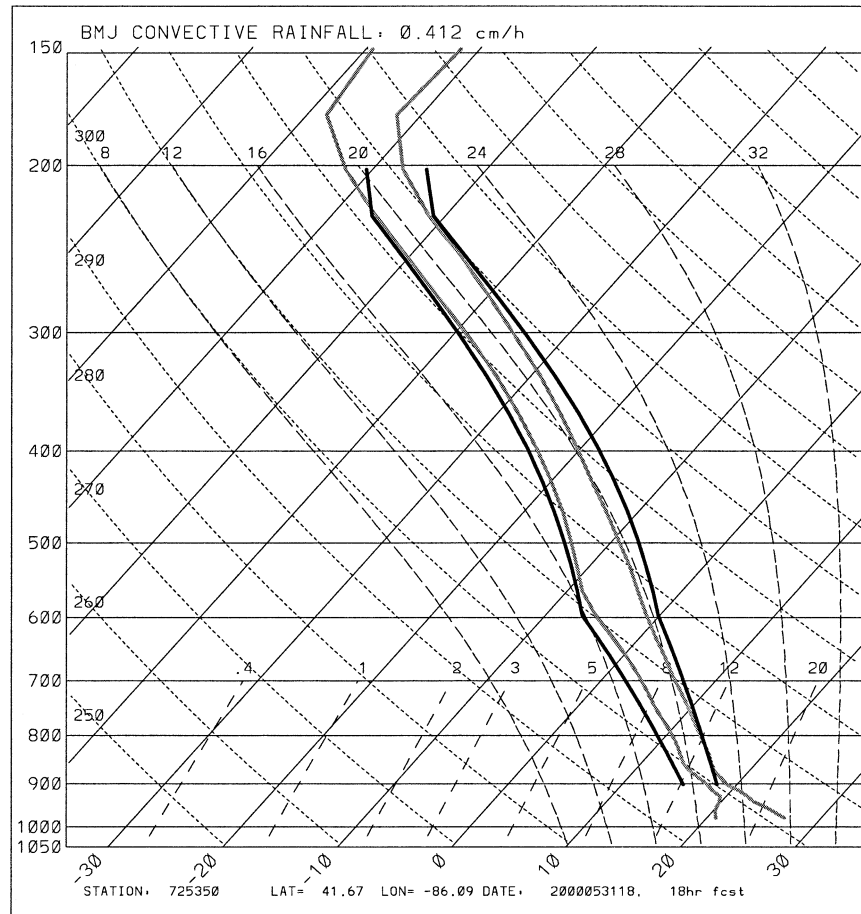


FIG. 3. As in Fig. 1 but for the final reference profiles, after adjustment to ensure enthalpy conservation.

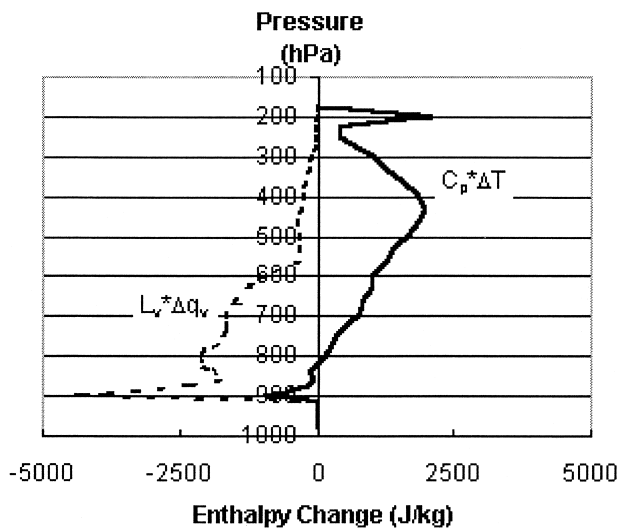


FIG. 4. As in Fig. 2 but for the final reference profiles, after adjustment to ensure enthalpy conservation.

the right-hand side were positive. Consider a sounding with the same thermal profile as shown in Fig. 1 but a 15% drop in relative humidity within the cloud layer (Fig. 5). The preliminary  $T_{ref}$  and  $q_{ref}$  profiles would be the same here as in Fig. 1, but, with the lower cloud-layer humidity, these preliminary profiles must be shifted farther to the left before enthalpy is conserved (Fig. 5). Once conservation is achieved, the curves have been moved so far over that  $\int_{p_b}^{p_t} C_p \Delta T dp < 0$  and  $\int_{p_b}^{p_t} L_v \Delta q dp > 0$  (Fig. 6). In other words, for the configuration of  $T_{ref}$  and  $q_{ref}$  specified by the BMJ scheme, enthalpy can only be conserved in this relatively dry sounding if there is a net *cooling* and *moistening* of the column! This would equate with a negative accumulation of precipitation, so deep convection would not be allowed.

This result shows that activation of deep convection with the BMJ scheme hinges on the presence of sufficient cloud-layer moisture. If we systematically change the cloud-layer relative humidity over a broad range, a nearly linear relationship between deep-layer moisture and parameterized BMJ rainfall emerges (Fig. 7). For a given temperature profile, the rainfall predicted by the

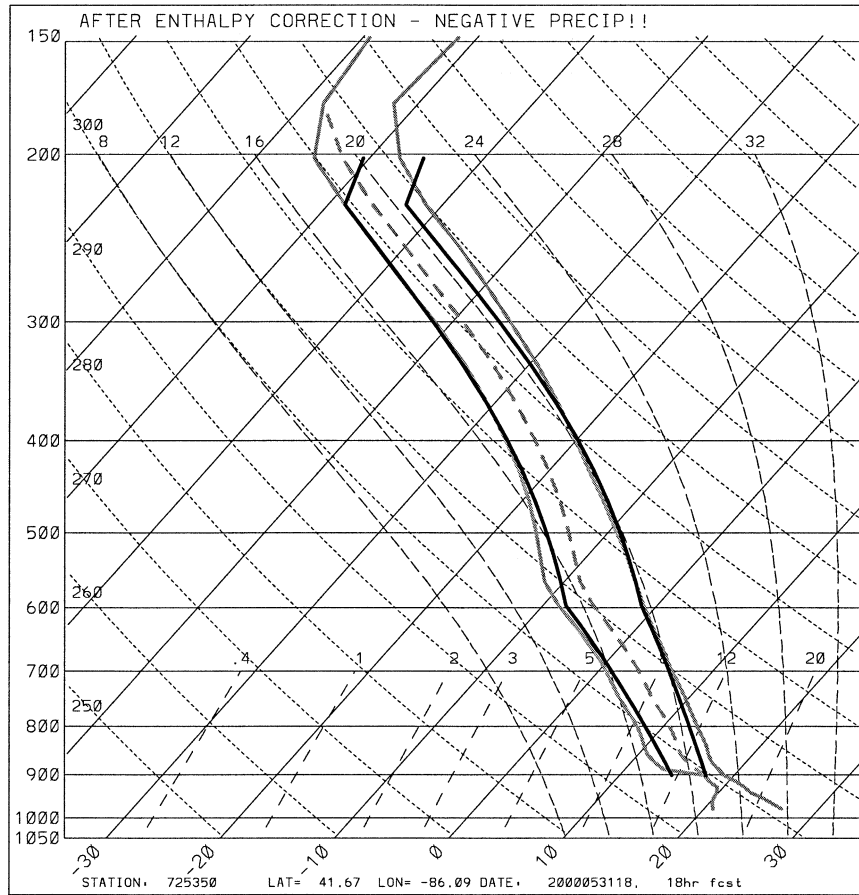


FIG. 5. As in Fig. 3 but with a modification to the original sounding. Light dashed line indicates the original dewpoint profile; light solid line indicates the new input dewpoint profile, obtained by decreasing relative humidity 15% in the cloud layer.

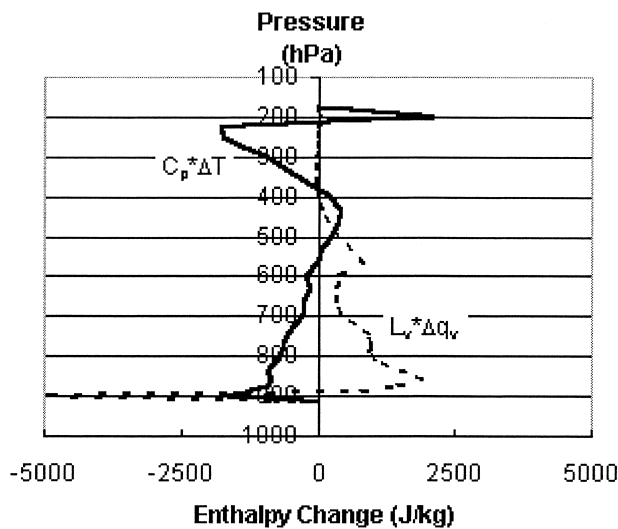


FIG. 6. As in Fig. 4 but with the drier sounding shown in Fig. 5 as input to the BMJ scheme.

scheme is very sensitive to cloud-layer relative humidity.

The BMJ scheme does not contain an explicit “trigger function” (Kain and Fritsch 1992). In particular, it does not evaluate explicitly whether incipient convective parcels can overcome a CIN layer to reach their level of free convection. Nonetheless, a CIN layer *does* inhibit the activation of BMJ *deep* convection in an implicit way because of the scheme’s constraints on enthalpy conservation, net heating in the column, and an increase in entropy. For instance, consider the situation of a strong inversion (examples of which can be found in Fig. 13a, described later). After enthalpy conservation is imposed, the BMJ reference profiles would typically introduce strong cooling and moistening within the inhibition layer. If this were not offset by stronger warming and drying elsewhere in the column, net heating and precipitation would be negative and deep convection would be aborted. Considerable cooling and moistening of the environment would be necessary, especially within the CIN layer, before the BMJ scheme would produce net heating and drying in this scenario, as required for activation. Thus, while not concerning itself with de-

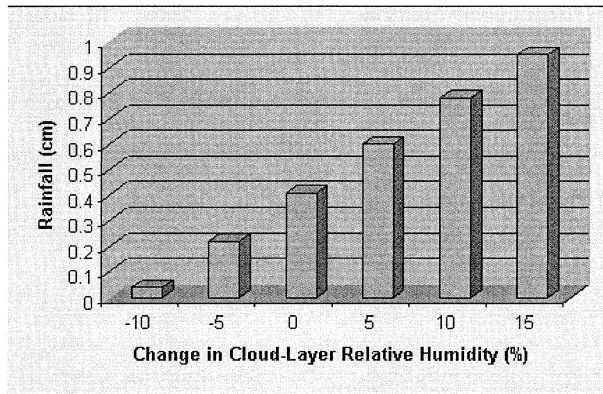


FIG. 7. Parameterized convective rainfall from the BMJ scheme as a function of cloud-layer relative humidity changes similar to those depicted in Fig. 5.

tailed structures and parcel buoyancy in the inhibition layer, BMJ deep convection is suppressed by relatively warm and dry layers in the model atmosphere.

When the model atmosphere is deemed too dry to support deep convection, the BMJ scheme attempts to generate shallow convection. The scheme can also revert to shallow convection if the computed reference profiles would introduce a negative *entropy* change (Janjić 1994), but in practice this restriction suppresses activation of deep convection much less frequently than does insufficient moisture in the sounding.

#### b. Shallow convection

The potential for shallow convection is evaluated when deep convection is aborted or computed cloud depth is less than 200 hPa. Cloud top is specified not as the EL, but as the layer within 200 hPa above cloud base in which the relative humidity drops off the fastest (Janjić 1994). The criterion is intended to identify the base of a stable layer where relatively warm and dry air inhibits further development of convective clouds that are rooted below. The shallow convection com-

ponent of the parameterization is designed to mix moisture up from cloud base to cloud top and to mix heat down from cloud top to cloud base. In practical terms, it parameterizes the effects of condensation around cloud base and evaporation near cloud top.

As with deep convection, the effects of shallow clouds are introduced by adjusting to reference profiles of temperature and moisture. These profiles are *not* based on observations of sounding modifications by deep convective activity; rather they are constructed on the basis of observed thermodynamic structures in non-precipitating cumulus regimes, for example, trade wind, stratocumulus, or “fair-weather” cumulus regimes. Observations suggest that vertical profiles in active shallow cloud layers resemble a “mixing line” between air from cloud top and cloud base in these regimes (Betts 1986). So, the first step is to generate a mixing line of temperature.

Model parcels from both cloud base and cloud top are lifted to their respective saturation points (i.e., their LCLs). The line connecting these two points is the mixing line. The slope of this line gives the slope of  $T_{ref}$ . The temperature of the input sounding at cloud base serves as the preliminary anchor point for  $T_{ref}$ , and the previously determined cloud top gives its vertical extent (Fig. 8). As with deep convection, the preliminary  $T_{ref}$  must be adjusted by shifting the entire profile to the right or left (but maintaining the slope). For shallow convection, this can be done independent of the moisture profile because the constraints are different. To be specific, shallow convection warms near cloud base and cools aloft, but the net heating *must be zero* (i.e., the latent heating of condensation is offset by latent cooling of evaporation). In other words, integrated over the cloud layer,  $C_p \Delta T = 0$ . For the sounding shown in Fig. 8, this adjustment amounts to shifting  $T_{ref}$  to the right (Fig. 9).

The reference moisture profile is determined in a similar manner. Determination of  $q_{ref}$  is based on the requirements that (a) the total amount of moisture within

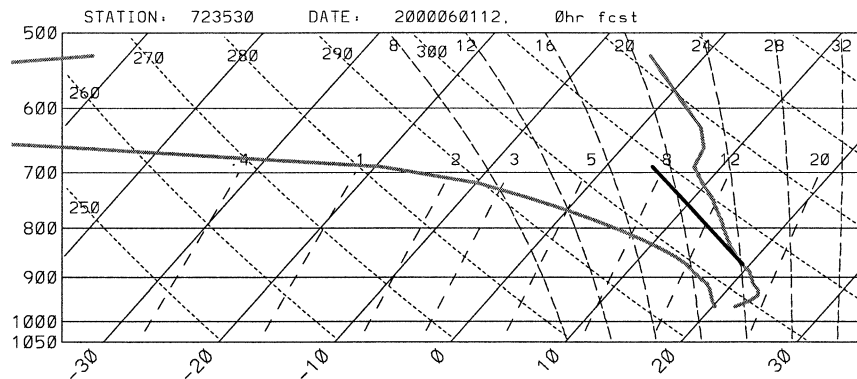


FIG. 8. Model initial condition (thick, light solid lines) and first-guess  $T_{ref}$  from the BMJ shallow convection component (thick, dark solid line), valid 1200 UTC 1 Jun 2000 at Oklahoma City, OK (KOKC).

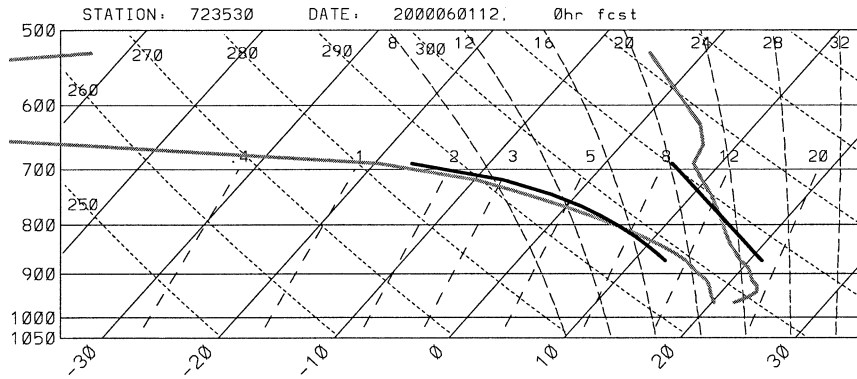


FIG. 9. Model initial condition (thick, light solid lines) and final  $T_{\text{ref}}$  and  $q_{\text{ref}}$  from the BMJ shallow convection component (thick, dark solid lines), valid 1200 UTC 1 Jun 2000 at KOKC.

the cloud remains unchanged and (b) the entropy change within the cloud is prescribed to be a small positive constant (which serves as a tuning parameter). These requirements provide two constraints that are sufficient to define the humidity profile, under the assumption that  $q_{\text{ref}}$  changes linearly as a suitably chosen function of pressure. Because  $q_{\text{ref}}$  is specified to change linearly as a function of reference temperature (Janjić 1994), the profile tails off sharply toward cloud top, when viewed on a skew  $T$ - $\log p$  diagram (Fig. 9), rather than paralleling  $T_{\text{ref}}$ . As with temperature, there can be no net change in  $q$  over the entire depth of the cloud, so drying near cloud base is exactly balanced by moistening below cloud top.

Several additional criteria are checked before shallow convection is activated (Janjić 1994): shallow convection is not allowed if  $T_{\text{ref}}$  results in upward transport of temperature,  $q_{\text{ref}}$  is supersaturated at any point,  $T_{\text{ref}}$  is superadiabatic,  $T_{\text{ref}}$  is isothermal,  $q_{\text{ref}}$  includes negative values of  $q$  at any point, or  $q_{\text{ref}}$  gives an increase in  $q$  with height. If any of these restrictions preclude activation, no convective feedbacks occur at the current grid point.

### c. Convective feedbacks

For both deep and shallow convection, convective feedbacks are introduced in the Eta Model as a temperature tendency,

$$\left. \frac{\partial T}{\partial t} \right|_{\text{conv}} = \frac{(T_{\text{ref}} - T)}{\tau_c}, \quad (2)$$

and a moisture tendency,

$$\left. \frac{\partial q}{\partial t} \right|_{\text{conv}} = \frac{(q_{\text{ref}} - q)}{\tau_c}, \quad (3)$$

where  $\tau_c$  is a convective timescale. The timescale can be as short as 50 min but may be considerably longer for deep convection depending, basically, on the precipitation rate and change in entropy (Janjić 1994). In

practice, the characteristic profiles associated with the scheme begin to emerge from initial soundings soon after the scheme is activated.

### 3. Effect of the convective scheme on forecast soundings

In this section, the effect of the BMJ scheme on model soundings is demonstrated. Specific model forecast soundings are shown, and a 1D, stand-alone, diagnostic version of the scheme is used to reproduce the reference thermodynamic profiles that the scheme would generate in a model forecast. The profiles and sequences of profiles demonstrated herein are typical of the scheme, but we choose to focus on unusual or problem cases, because these cases present the greatest sounding interpretation challenges for forecasters.

#### a. A case of shallow convection only

On 11 May 2000, Birmingham, Alabama, (BMX) experienced fair weather and partly cloudy skies. At 1200 UTC, observations showed a fairly moist sounding below 800 hPa but a very dry and stable atmosphere above. Initial conditions from the Eta Model valid at this time showed good agreement with observations (Fig. 10a). The BMJ scheme located the most unstable (highest  $\theta_e$ ) air at about 900 hPa and determined that this air possessed some CAPE in the layer above 600 hPa. Deep convection was not allowed because this CAPE layer was too dry, but shallow convection was activated. The scheme placed cloud base near 880 hPa, the approximate LCL of the highest- $\theta_e$  air. It located the highest lapse rate of relative humidity at about 800 hPa, thus designating this level as the shallow cloud top. (Note that there was actually no CAPE within the shallow cloud layer!) The scheme computed a reference temperature profile with a steeper lapse rate than the environment, introducing a warming tendency in the lower half of the cloud layer and cooling in the upper half (Fig. 10b). At the same time, it introduced weak drying

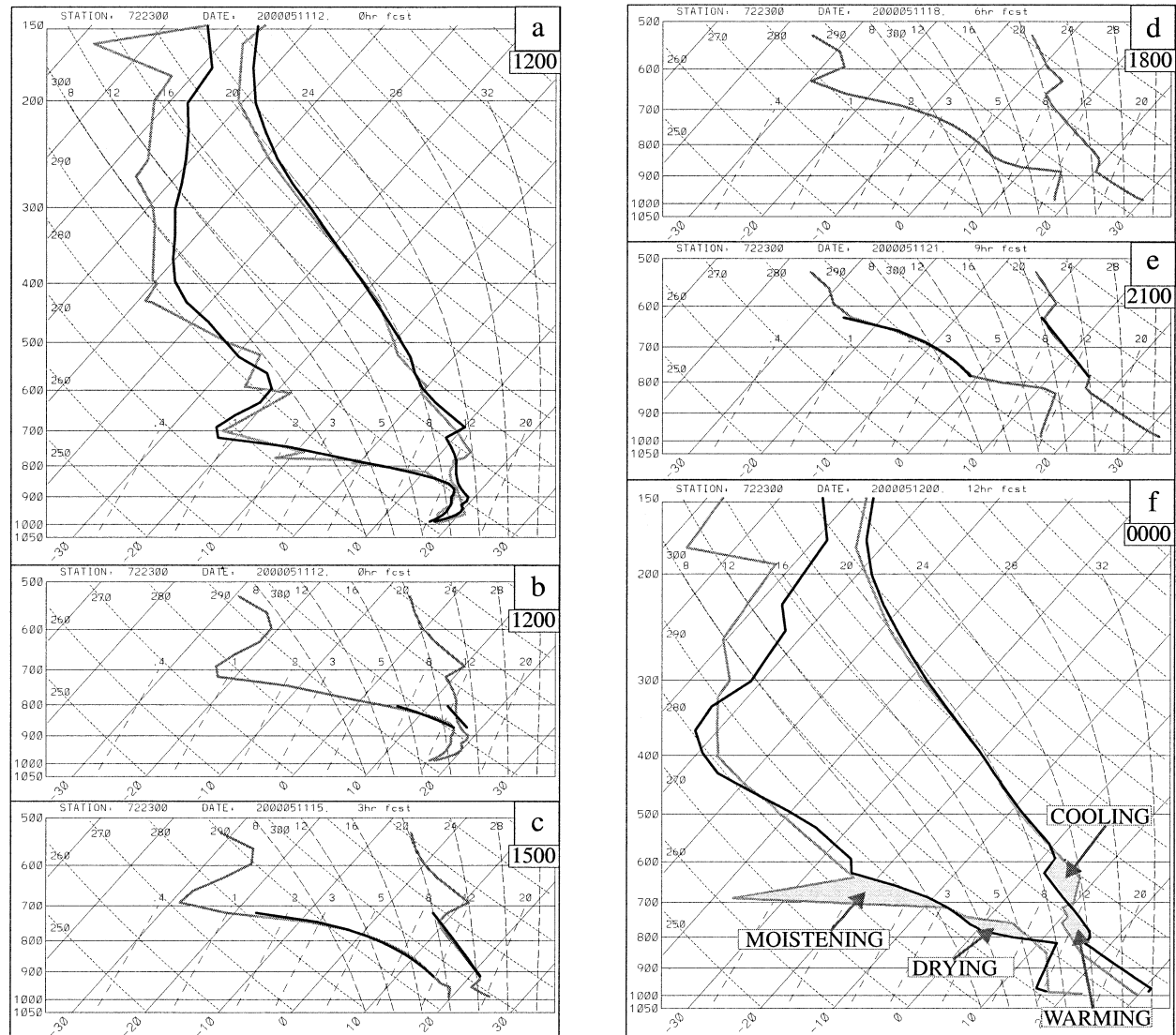


FIG. 10. A sequence of Eta Model forecast soundings valid from 1200 UTC 11 May to 0000 UTC 12 May 2000 over Birmingham, AL (BMX). (a) Model initial condition (thick dark curves) overlying the observed sounding (thick light curves); (b) BMJ shallow-convection reference profiles (thick dark curves) overlying the model 0-h forecast (initial condition); (c) as in (b) but for the 3-h forecast, valid 1500 UTC; (d) model 6-h forecast, valid 1800 UTC; (e) as in (b) but for the 9-h forecast, valid 2100 UTC; and (f) as in (a) but with the model 12-h forecast, valid 0000 UTC 12 May, overlying the observed sounding. Shading in (f) highlights the changes in temperature and moisture associated with the BMJ scheme.

in the lower part of the layer and weak moistening in the upper part. Note the distinctly smooth character of the reference profiles for both temperature and moisture.

Diagnostic evaluation at hours 1–3 (1300–1500 UTC) indicated that the shallow component of the scheme was active at each of those times and, judging from the 1500 UTC sounding structure, that it was probably active continuously during this period (Fig. 10c). This sounding shows a monotonic decrease in both  $T$  and  $q$  between about 920 and 740 hPa. By this time, solar heating had warmed the boundary layer so that convection had become surface based and the LCL (cloud base) had dropped from about 880 (3 h earlier) to 920 hPa. Con-

vective tendencies from the scheme had apparently contributed to substantial warming near cloud base, and significant cooling had occurred between about 740 and 800 hPa, apparently associated with cloud-top cooling tendencies imposed by the scheme (cf. Figs. 10b,c).

At this time,  $T_{\text{ref}}$  introduced strong cooling tendencies just above the base of the inversion (Fig. 10c), and the evolution of the profiles over time suggests that similar cloud-top cooling tendencies had eroded the stable layer that initially existed between about 750 and 850 hPa. This process also strengthened the inhibition layer above. Over the same time period, the convective tendencies had apparently contributed to strong drying in

the layer from about 800 to 920 hPa. If parameterized convective tendencies alone were active, we would also see moistening near cloud top, but large-scale subsidence was occurring, and the drying tendencies associated with this process apparently offset the convective moistening. Note that the shallow cloud depth is about 200 hPa, the maximum depth allowed by the scheme.

The 1800 UTC sounding still shows the "footprint" of the BMJ scheme (Fig. 10d), but a diagnostic check at this time reveals that shallow convection was not activated. Instead, the scheme aborted at this point because adjustment to computed reference profiles would have produced an upward transport of temperature. The concept of rejecting points where the reference profile would result in an upward transport of heat is discussed in some detail in Janjić (1994). There unfortunately are no readily discernible sounding characteristics that would allow us to identify, with a quick visual inspection, points where the BMJ scheme would abort. By performing diagnostic checks with a higher time frequency, we have found that small changes in sounding structures can make the difference between activation and abortion by the temperature transport check, so that individual grid points often activate intermittently as the computed temperature changes hover near zero. The persistence of the BMJ footprint in BMX soundings suggests that the scheme has been active at least intermittently between 1500 and 1800 UTC.

The scheme was active at 2100 UTC, though it was aborted an hour earlier, suggesting that it still may have been in an intermittent mode. Shallow convective adjustment profiles differ very little from the input sounding (Fig. 10e), suggesting that the scheme was maintaining existing sounding structures but no longer introducing significant changes.

By 0000 UTC 12 May, the effect of 12 h of BMJ shallow convection can be inferred by comparison of the model forecast sounding with the observed sounding (Fig. 10f). The characteristic footprint of the scheme can be seen in the 600–800-hPa layer. In terms of the temperature profile, the CIN layer near 700 hPa was distorted by the scheme. Warming near the base of parameterized clouds has apparently introduced an anomalous stable layer near 800 hPa while cooling near cloud top apparently induced an isothermal layer in the sounding near 600 hPa. In effect, the observed strong CIN layer near 700 hPa has split into two weaker CIN layers near the base and top of the parameterized shallow cloud. The moisture profile is distorted in a consistent way. In particular, it appears that the scheme has dried the lower part of the cloud layer and moistened the middle and upper parts.

The character of the temperature and moisture anomalies shown in this case is consistent with our routine examination of forecast soundings at the National Severe Storms Laboratory (NSSL) and the Storm Prediction Center (SPC). Although it is not so obvious here, the anomalies associated with parameterized shallow

convection are often communicated to the boundary layer as well. In particular, when shallow cloud base is near the top of the boundary layer, parameterized turbulent diffusion in the model has a tendency to take anomalously warm and dry air near the top of the boundary layer and mix it downward. All of these effects have a significant impact on the values obtained in computation of CAPE, CIN, and other diagnostic quantities.

*b. A case of shallow convection making a transition to deep convection*

On 24 April 2001, a vigorous upper-level short-wave trough was lifting northeastward across the Great Lakes toward the northeastern states. An associated deep surface low over Quebec was also moving to the northeast. Trailing southwestward from this low was a surface cold front. This front extended along the Appalachians into the southeastern United States. The front was advancing slowly eastward over the Mid-Atlantic states into a region of moderate instability over the Carolinas and Virginia. The upper-level forcing associated with this front was weak.

The model initial (1200 UTC) condition at Greensboro, North Carolina, (GSO) showed good agreement with observations (Fig. 11a). The sounding was nearly saturated above about 300 hPa, was relatively dry through midlevels, and was very moist below 800 hPa. The BMJ scheme determined that no CAPE existed for parcels rooted in the lowest 200 hPa, so no convection was activated at this time. CAPE continued to be absent through 1400 UTC, but solar heating led to the development of some instability during the following hour. By 1500 UTC, the scheme had clearly placed its footprint on the sounding as evidenced by a sharp stable layer at 920 hPa, a monotonic decrease in temperature ending abruptly at about 740 hPa, and a smooth convex moisture profile over the same layer (Fig. 11b). Reference profiles from the scheme confirm the character of this influence. Once again the scheme was acting over the maximum allowable depth of 200 hPa. It is not allowed to extend the shallow cloud layer any higher.

The character of the scheme's influence changed little over the next 2 h (1500–1700 UTC). In particular, thermodynamic profiles within the shallow cloud layer retained the same shape, although solar heating caused cloud base to rise with time, which also allowed cloud top to rise (Fig. 11c). By 1800 UTC, low-level convergence associated with the advancing cold front was very strong (not shown) and boundary layer depth was increasing rapidly. Boundary layer moisture was not decreasing significantly as the layer deepened, suggesting the presence of strong moisture convergence. At the same time, there was little if any upward motion aloft.

Because the computed shallow cloud base was near the top of the boundary layer, the scheme effectively transported moisture from the top of the well-mixed

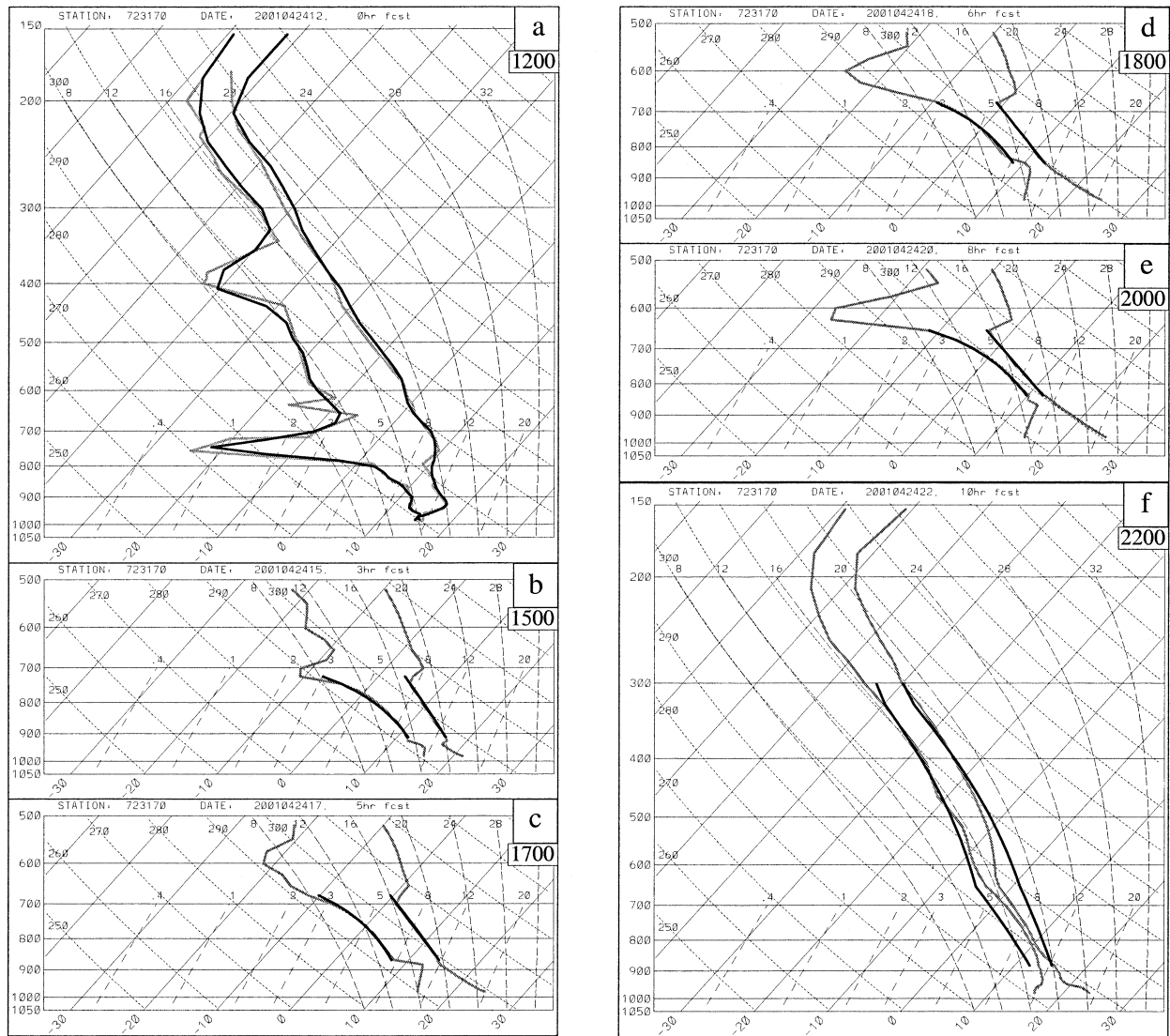


FIG. 11. A sequence of Eta Model forecast soundings valid from 1200 to 2200 UTC 24 Apr 2001 over Greensboro, NC (KGSO). (a) Model initial condition (thick dark curves) overlying the observed sounding (thick light curves); (b) BMJ shallow-convection reference profiles (thick dark curves) overlying the model 3-h forecast, valid 1500 UTC; (c) as in (b) but for the 5-h forecast, valid 1700 UTC; (d) as in (b) but for the 6-h forecast, valid 1800 UTC; (e) as in (b) but for the 8-h forecast, valid 2000 UTC; and (f) as in (b) but for the 10-h forecast, valid 2200 UTC, and with BMJ *deep* convection profiles.

layer (or just above the top) into the lower-to-middle part of the shallow cloud layer (Fig. 11d). Note the substantial moistening of the shallow cloud layer between 1700 and 1800 UTC (cf. Figs. 11c,d). At the same time, shallow convection was effectively communicating with the convective boundary layer (through turbulent diffusion), removing moisture from low levels. This communication between parameterized boundary layer turbulence and shallow convection is frequently reflected in Eta Model simulations, as noted in the previous section.

Between 1800 and 2000 UTC, boundary layer depth begins to peak. Parameterized shallow convection continues to moisten the cloud layer and cool its upper half.

Yet, above about 650 hPa, the atmosphere remains dry, precluding the development of parameterized deep convection (Fig. 11e). After 2000 UTC, upward motion commences aloft within the model, and BMJ deep convection activates between 2100 and 2200 UTC. By the latter time, the remnants of the shallow convective structures are still evident, but it can be seen that the sounding is evolving toward the familiar BMJ deep convective reference profiles (Fig. 11f), in which the temperature profile is slightly less stable than moist adiabatic and the moisture profile is subsaturated with a dewpoint depression that varies linearly from about 3°C at cloud base to ~7°C at the freezing level and back to ~4°C at cloud top.

*c. A transition from shallow convection to “shallow” deep convection*

At 1200 UTC on 23 April 2001, an intense upper low was located over the upper Mississippi River valley and was forecast to move northeastward to a position over western Lake Superior over the next 12 h. An associated surface low was expected to track just to the east of the upper low, with a strong trailing cold front surging eastward through eastern Wisconsin. Convective instability ahead of the cold front was marginal ( $\text{CAPE} \approx 1000 \text{ J kg}^{-1}$ ), but strong vertical wind shear and dynamic forcing for upward vertical motion alerted forecasters to the possibility of severe convection in this area.

A line of showers had just moved through Green Bay, Wisconsin, (GRB) at 1200 UTC, and the Eta Model initial condition reflected this scenario, with a very moist sounding through the mid- to upper troposphere but subsaturation below about 600 hPa (Fig. 12a). Although some CAPE existed at this time, the scheme aborted because of a negative entropy change, so it did not activate at the initial time.

By 1400 UTC, a “dry slot” had moved in over the region and midlevel drying was occurring in the model. Smaller-scale vertical structures had essentially disappeared from the model sounding between about 650 and 850 hPa (cf. Figs. 12a,b), suggesting the influence of BMJ shallow convection in this layer. BMJ reference profiles at this time corroborate this impression, revealing active shallow convective tendencies in the layer from about 690 to 840 hPa (Fig. 12b). Judging from the thermodynamic profile and the location of cloud base, it appears that the scheme was using air from about 870 hPa as the “source” air for the updraft.

An hour later (1500 UTC), a shallow convective boundary layer had developed and shallow convection became surface based (Fig. 12c). The formation of a new shallow convective layer could be discerned from changes in the sounding structure and parameterized feedbacks over the 790–930-hPa layer (Fig. 12c). Note also that dry air had continued to move in aloft.

Over the next 2 h, the boundary layer continued to warm and to moisten. Shallow convection remained active in the layer from just above 800 hPa to just below 900 hPa (Fig. 12d). Because the boundary layer moistened as it warmed, cloud base did not rise, and cloud top remained nearly constant because a sharp moisture gradient was maintained just above 800 hPa. Because the shallow scheme necessarily warms near cloud base and cools near cloud top, lapse rates in the shallow cloud layer increased with time. Likewise, with moisture being continuously replenished near cloud base, the shallow cloud layer moistened with time (cf. Figs. 12c,d).

By 1800 UTC, the 800–900-hPa layer was nearly saturated and the lapse rate was close to dry adiabatic (Fig. 12e). Shallow convection was aborted at this time because it would have resulted in upward transport of

temperature, though a superadiabatic reference profile probably would have caused it to abort even if it had passed the upward temperature transport test. The “stair-step” appearance to the thermodynamic profiles is likely due to imbalances between grid-resolved condensation [the condensation process begins at  $\approx 80\%$  relative humidity (Zhao et al. 1997)] and turbulent vertical diffusion.

After 1800 UTC, suppression of deep convection continued because of the dry air aloft, and parameterized shallow convection was inhibited by high lapse rates (recall that the scheme requires that  $T_{\text{ref}}$  introduce a warming tendency in the lower half of the shallow cloud layer and a cooling tendency in the upper half, yet it *aborts* if  $T_{\text{ref}}$  is superadiabatic), so the scheme effectively shut down for several hours. By 2200 UTC a superadiabatic, nearly saturated layer had developed between the surface and about 800 hPa (Fig. 12f). The remedy for this problematic structure arrived within the next hour in the form of surface cooling. As the surface began to cool, the moist adiabat associated with lifting of a surface-layer parcel moved to the left on a skew  $T$ - $\log p$  diagram. As a consequence, although the EL for a surface-based parcel was about 350 hPa at 2200 UTC, by 2300 UTC it had dropped to about 700 hPa (cf. Figs. 12f,g). With this latter cloud top, most of the very dry air aloft was excluded from the cloud layer, yet the computed cloud depth still exceeded the minimum value of 200 hPa for deep convection. So, deep convection was activated (Fig. 12g), and by 0000 UTC the model had eliminated the unrealistic moist superadiabatic structure (Fig. 12h).

The evolution of model soundings that occurred at GRB on this day was unusual. The BMJ scheme rarely allows such structures to develop. On occasion, however, the atmosphere produces meteorological conditions that “slip through the cracks” of the criteria that are used to activate the BMJ scheme. Although this inactivity of the scheme is typically temporary, it can allow unrealistic and atypical vertical structures to develop, causing confusion among those who are trying to interpret model behavior.

*d. A spurious transition from shallow to deep convection*

On 20 April 2001, a vigorous short-wave trough was expected to lift out from the southwestern United States through the central Rockies and eventually across the northern plains. Instability was widespread across the central and southern plains, and forecasters at SPC were concerned about the possibility of severe thunderstorms with this system. Convective instability was strongest over the southern plains, but CIN was also very high in this region. Furthermore, dynamic forcing for upward vertical motion was expected to be concentrated to the north, providing forecasters with good reason to believe that the CIN layer would maintain its suppression of

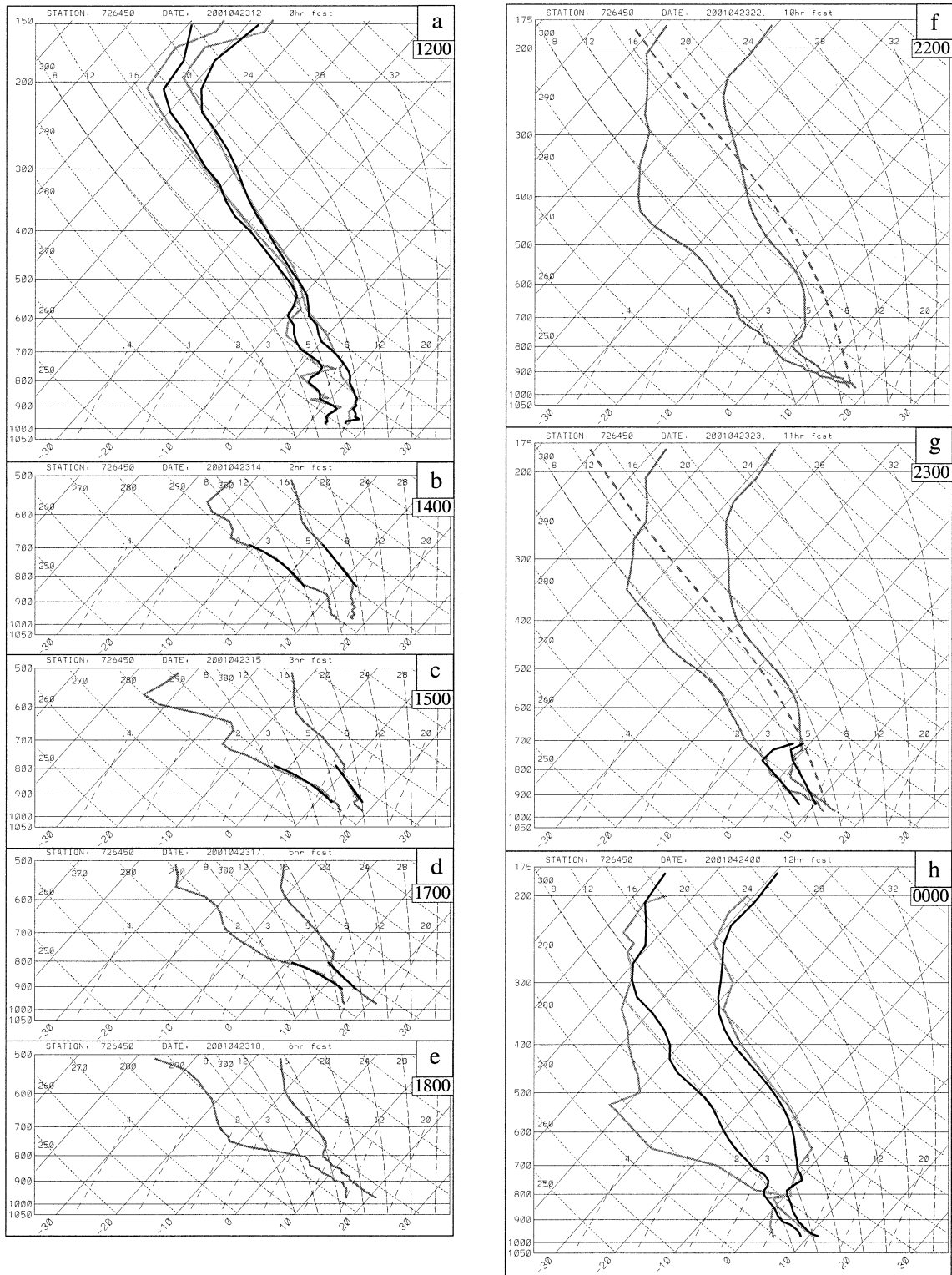


FIG. 12. A sequence of Eta Model forecast soundings valid from 1200 UTC 23 Apr to 0000 UTC 24 Apr 2001 over Green Bay, WI (GRB). (a) Model initial condition (thick dark curves) overlying the observed sounding (thick light curves); (b) BMJ shallow-convection reference profiles (thick dark curves) overlying the model 2-h forecast, valid 1400 UTC; (c) as in (b) but for the 3-h forecast, valid 1500 UTC; (d) as in (b) but for the 5-h forecast, valid 1700 UTC; (e) model 6-h forecast, valid 1800 UTC; and (f) model 10-h forecast, valid 2200 UTC, with thick dashed curve indicating the reference moist adiabat computed by the BMJ scheme; (g) BMJ deep-convection reference profiles (thick dark curves) overlying the model 11-h forecast, valid 2300 UTC, with thick dashed curve indicating the reference moist adiabat computed by the BMJ scheme; and (h) as in (a) but with the model 12-h forecast, valid 0000 UTC 24 Apr, overlying the observed sounding.

convective initiation over the southern plains. Nonetheless, 3000–4000 J kg<sup>-1</sup> of CAPE was expected to be in place over north-central Texas and much of Oklahoma and wind fields were favorable for organized severe convection, *provided that convection could develop*. Moreover, the 0000 UTC 20 April run of the Eta Model developed convection over southern Oklahoma and northeastern Texas by 0000 UTC 21 April. Thus, forecasters at the SPC were compelled to examine closely the evolution of Eta Model soundings over this region.

The initial model sounding from the Dallas–Fort Worth, Texas, (FWD) area, valid 0000 UTC 20 April, showed fairly good agreement with observations, though the strength of the CIN layer was underestimated in the model initial condition (Fig. 13a). BMJ deep convection was not allowed because of the dry air aloft, but shallow convection activated immediately. By the end of the first hour (0100 UTC), shallow convective tendencies had apparently modified the sounding considerably, but the detailed vertical structures in this environment were still far from the smooth shallow convective reference profiles (Fig. 13b). Within a few hours after this time, surface cooling lowered  $\theta_e$  values to the point at which parcel buoyancy became marginal. During the ensuing nighttime hours, shallow convection activated intermittently and with little consistency in cloud base, cloud top, or cloud depth (not shown).

By 1200 UTC, it was not possible to identify clearly a single shallow convective layer or the characteristic structures imposed by BMJ shallow convection. Nonetheless, comparison of the 12-h forecast sounding with the observed sounding suggests that the scheme had been very effective at performing its primary function—transporting heat downward and moisture upward. In particular, this effect is suggested by the presence of anomalously warm and dry air in the model sounding between about 820 and 920 hPa (Fig. 13c).

The effect of the scheme became easier to track after surface heating provided some buoyancy for surface-based parcels after 1500 UTC. By 1600 UTC, *deep* convection was still not allowed, but shallow convection became surface based and began to modify a relatively shallow layer, from about 860 to 950 hPa (Fig. 13d). As the scheme moistened successively higher layers near its cloud top, the sharpest vertical gradient in relative humidity shifted upward, causing the computed cloud top to rise (see section 2b). By 1700 UTC, cloud top moved up to almost 800 hPa, and the reference temperature profile was much cooler than the input sounding near cloud top and was considerably warmer near cloud base (Fig. 13e). By 1800 UTC, shallow convective tendencies had apparently introduced a substantial cold anomaly near and just above 800 hPa and convective tendencies were acting to expand this anomaly to higher levels (Fig. 13f), but 1 h later shallow cloud depth had fallen back to about 500 m (Fig. 13g). This jump was apparently caused by the redevelopment

of a strong vertical gradient of relative humidity near 850 hPa. Characteristic profiles associated with the new shallow cloud layer had been clearly etched into the model sounding at this time in the 850–900-hPa layer.

A deeper shallow cloud reestablished itself by 2100 UTC, and shallow convective tendencies continued to chip away at the stable layer in the lower-to-middle troposphere (Fig. 13h). The scheme produced shallow cloud layers of varying depth through 0000 UTC 21 April, so that all remnants of the CIN layer that initially existed near 800 hPa were effectively eliminated from the sounding. In reality, however, a strong capping inversion remained over FWD (Fig. 13i). The BMJ scheme activated deep convection shortly after 0000 UTC, although thunderstorms never developed over this area during this event. By 0100 UTC, the FWD forecast sounding exhibited the characteristic structures of BMJ deep convection (Fig. 13j), but deep convection had already turned off because of negative entropy change.

The evolution of model soundings at FWD was problematic, but the model suggested that any deep convection at FWD would be weak and short lived. At nearby grid points, however, the deviation from reality was much more dramatic and ominous. For example, the model generated an extremely unstable sounding *after* activating deep convection at the 23-h forecast time (2300 UTC) at Ardmore, in south-central Oklahoma (Fig. 14). Surface-layer parcels in this sounding had CAPE values over 4000 J kg<sup>-1</sup>—an *increase* from preconvective values.

For comparison, Fig. 14 also shows a 24-h forecast from an experimental configuration of the Eta Model used for daily forecasting at NSSL and SPC (Kain et al. 2001). This version of the model uses initial conditions that are identical to the operational Eta run, but it uses the Kain–Fritsch convective parameterization (Kain and Fritsch 1993) instead of the BMJ scheme. This scheme also parameterizes shallow convection, but it requires CAPE in the shallow cloud layer. Because of this requirement, shallow convection was mostly inactive in this parallel run. As a result, the model retained the strength and configuration of the capping inversion very well.

Forecasters at SPC have become skillful at interpreting the behavior of the BMJ scheme, and they took notice of the Eta forecast soundings during the overnight hours of 19–20 April, prior to the onset of this event (R. Thompson 2001, personal communication).<sup>1</sup> They considered this behavior within the context of the larger-scale environment. Furthermore, they took into consideration alternative sources of numerical guidance, such as the parallel Eta forecast using the Kain–Fritsch parameterization. In spite of the high *conditional probability* of severe weather (i.e., the probability that convection would become severe *if* thunderstorms devel-

<sup>1</sup> Richard Thompson is a lead forecaster for the SPC. He was working the 0000–0800 LT shift on 20 April 2001.

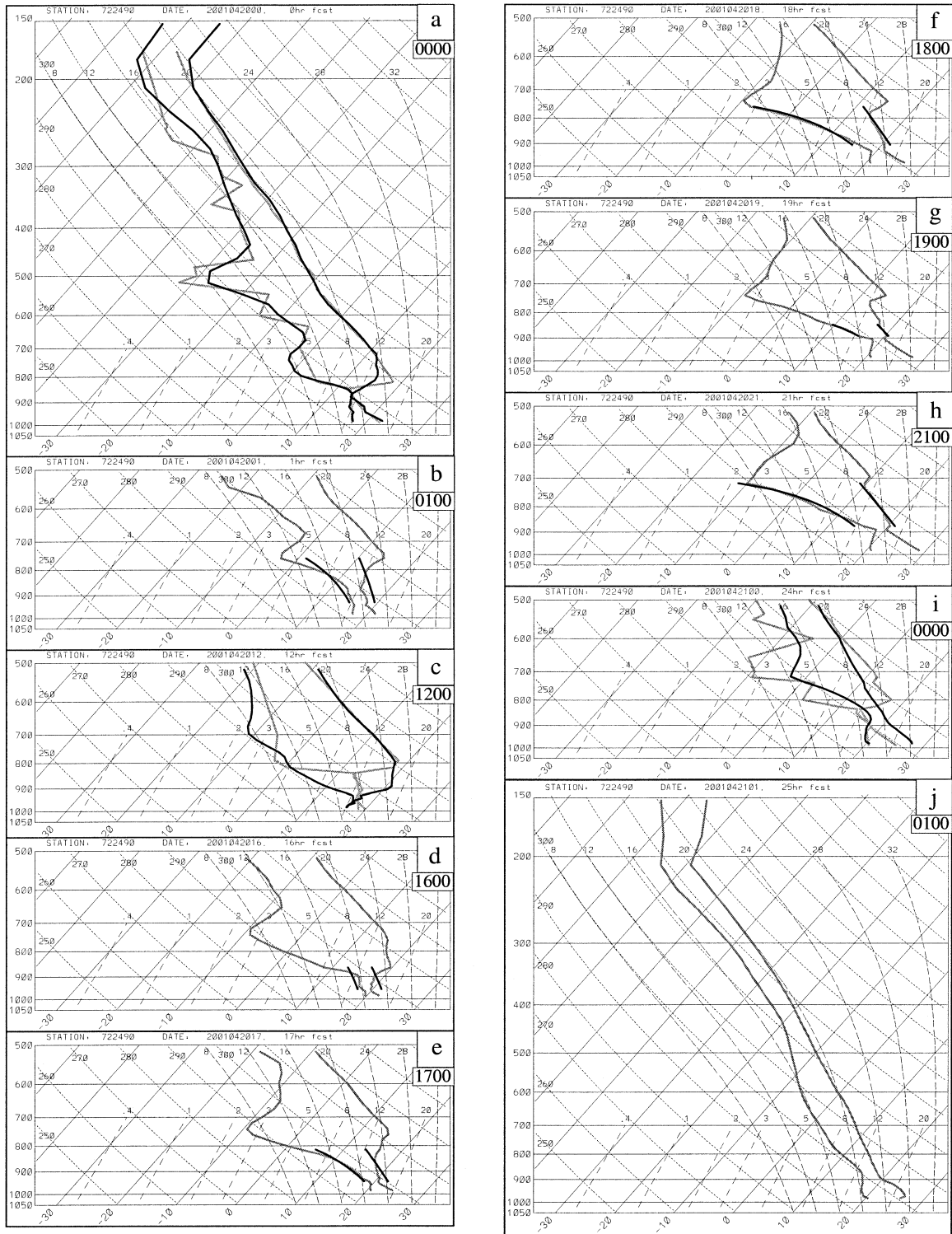


FIG. 13. A sequence of Eta Model forecast soundings valid from 0000 UTC 20 Apr to 0000 UTC 21 Apr 2001 over Dallas–Fort Worth (FWD). (a) Model initial condition (thick dark curves) overlying the observed sounding (thick light curves); (b) BMJ shallow-convection reference profiles (thick dark curves) overlying the model 1-h forecast, valid 0100 UTC; (c) as in (a) but for the 12-h forecast, valid 1200 UTC, overlying the observed sounding; (d) as in (b) but for the 16-h forecast, valid 1600 UTC; (e) as in (b) but for the 17-h forecast, valid 1700 UTC; (f) as in (b) but for the 18-h forecast, valid 1800 UTC; (g) as in (b) but for the 19-h forecast, valid 1900 UTC; (h) as in (b) but for the 21-h forecast, valid 2100 UTC; (i) as in (a) but for the 24-h forecast, valid 0000 UTC 21 Apr; overlying the observed sounding; and (j) model 25-h forecast, valid 0100 UTC 21 Apr.

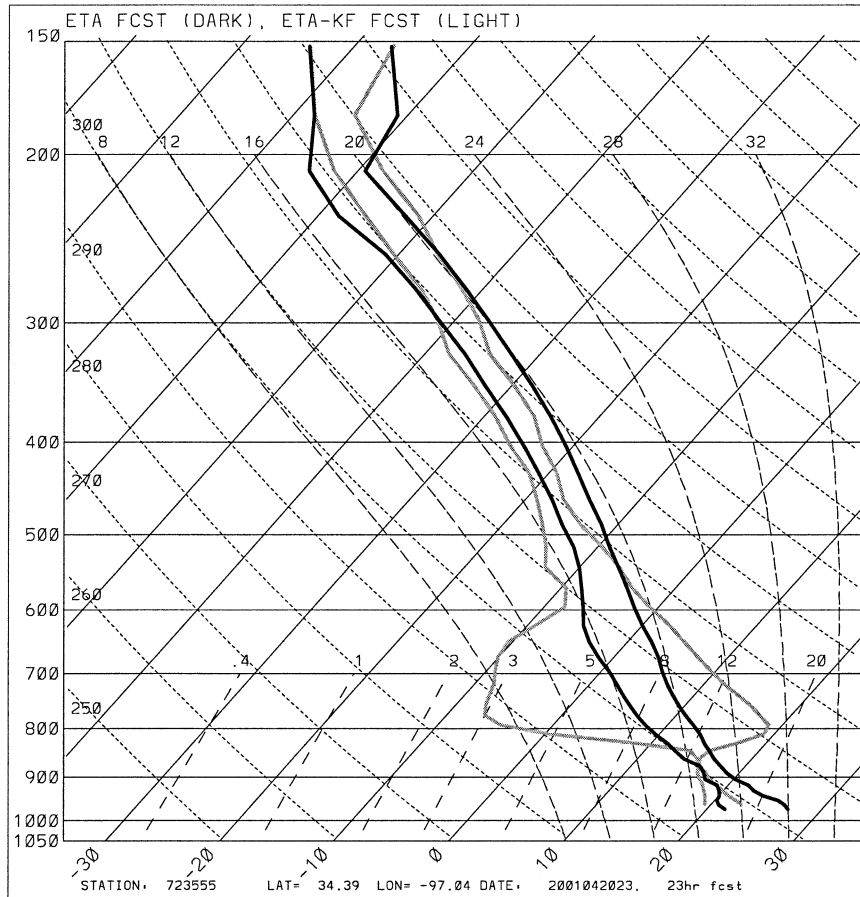


FIG. 14. Eta Model forecast sounding (thick dark curves) overlying a model forecast sounding from an experimental configuration of the Eta Model that uses the Kain-Fritsch convective parameterization in place of the BMJ scheme (thick light curves). Both soundings come from 23-h forecasts valid 2300 UTC 20 Apr 2001 over Ardmore, OK.

oped) and the activation of convection in the Eta Model, they issued a very low probability of severe weather over the southern plains. No thunderstorms developed over this area.

#### 4. Summary and discussion

All convective parameterizations contain arbitrary parameter settings and have characteristic behaviors that are sometimes inconsistent with reality. So, this study is not intended to single out the BMJ scheme as somehow inferior or inadequate. On the contrary, this scheme has been critically important to the success of the Eta Model running at the National Centers for Environmental Prediction (NCEP) and its enduring status as the primary 1–2-day operational forecast model in the United States. Other convective parameterizations have been tested in the Eta Model but none has produced consistently higher QPF verification scores than the BMJ scheme.

At the same time, the BMJ scheme is particularly amenable to critical examination because the shape and

character of its footprint are much easier to identify than characteristic profiles produced by other schemes—and there is value in knowing when and where a convective parameterization has been active in a model! Most important, a detailed examination of BMJ behaviors is warranted because model forecast soundings from the Eta Model have come to play an important role in preparing forecasts for many kinds of weather.

Forecasters concerned about thunderstorm development can benefit from knowing how to identify when parameterized *shallow* convection has been active. The BMJ shallow component warms and dries model layers near the LCL while cooling and moistening the model sounding near the computed cloud top. It nudges the environment toward profiles characterized by linear decreases in potential temperature  $\theta$  and  $q$  as a function of decreasing pressure. Oftentimes this process distorts the shape and structure of the CIN layer, sometimes completely eliminating a stable layer that can be critical for inhibiting convective development. This tendency can be very evident over the Great Plains of the United States, where elevated mixed layers create strong cap-

ping inversions with some regularity during the warm season (Carlson et al. 1983; Lanicci and Warner 1991). When the LCL is close to the top of a convective boundary layer, within which turbulent mixing is parameterized separately in the model, the combination of convection and turbulence parameterizations can effectively mix moisture out of the boundary layer up toward the shallow cloud top while mixing high- $\theta$  air downward into the boundary layer. When some or all of these processes are active in the model, convective parameters such as CAPE and CIN are significantly affected. If forecasters can learn to identify these characteristic tendencies associated with BMJ shallow convection, they can make more informed assessments of the likelihood of convective initiation and intensity.

It is also important for forecasters to be able to recognize when BMJ deep convection has been active. Unlike parameterized shallow convection, deep convective activity is easy to confirm by examining the convective rainfall field. Its characteristic thermodynamic profiles are also easy to recognize. The temperature profile is slightly unstable from cloud base to the freezing level and is then marginally stable (lapse rate slightly less than moist adiabatic) up to the computed cloud top. The dewpoint depression is specified to vary linearly from about 3°–5°C at cloud base to 7°–9°C at the freezing level and back to 3°–5°C at cloud top. As with the shallow convective signature, the active convective layer is often first recognizable by its characteristic lack of small-scale structure. Small-scale vertical structures in both the temperature and moisture fields are transformed quickly into curves with a nearly monotonic decrease in temperature and dewpoint with height when either deep or shallow convection activates with the BMJ scheme.

It is hoped that this study will promote the direct analysis of model forecast soundings, rather than relying on 2D plan-view plots of diagnosed quantities such as CAPE or CIN. Not only should this analysis help in removing ambiguity about how such fields are computed [which parcel was lifted, whether or not the virtual temperature correction (Doswell and Rasmussen 1994) was used, etc.], but it will also lead to better understanding of the characteristic behaviors of the BMJ scheme. Examination of model forecast soundings can provide valuable clues to help forecasters to comprehend and interpret overall model behavior. Yet, these soundings must always be used with caution. Developing a more complete understanding of the BMJ scheme can help forecasters to distinguish between those characteristics of model soundings that have a meteorological origin and those that are more of a computational anomaly.

*Acknowledgments.* This work was partially funded by a COMET Cooperative Project, UCAR Award 099-15805, and NOAA–University of Oklahoma Cooperative Agreement NA17RJ1227. This manuscript was

inspired by many conversations on the topic of convective parameterization between the authors and numerous scientists and forecasters at SPC and NSSL, often held during daily informal NSSL/SPC map discussions. In addition, the authors acknowledge COMET for its support, and especially for providing the first two authors several opportunities to discuss this topic with NWS forecasters at COMET training symposia. We are also grateful to Dr. Zavisla Janjić of NCEP/EMC for his comments and suggestions that helped greatly in clarifying and improving several aspects of the paper. The authors also thank Dr. Louis Wicker (NSSL), Dr. Kimberly Elmore (CIMMS/NSSL), and three anonymous reviewers for their constructive comments and helpful suggestions.

#### REFERENCES

- Betts, A. K., 1982: Saturation point analysis of moist convective overturning. *J. Atmos. Sci.*, **39**, 1484–1505.
- , 1986: A new convective adjustment scheme. Part I: Observational and theoretical basis. *Quart. J. Roy. Meteor. Soc.*, **112**, 677–691.
- , and M. Miller, 1986: A new convective adjustment scheme. Part II: Single column tests using GATE wave, BOMEX and arctic air-mass data sets. *Quart. J. Roy. Meteor. Soc.*, **112**, 693–709.
- Black, T. L., 1994: The new NMC Mesoscale Eta Model: Description and forecast examples. *Wea. Forecasting*, **9**, 265–278.
- Carlson, T. N., S. G. Benjamin, G. S. Forbes, and Y.-F. Li, 1983: Elevated mixed layers in the regional severe storm environment: Conceptual model and case studies. *Mon. Wea. Rev.*, **111**, 1453–1474.
- Doswell, C. A., III, and E. N. Rasmussen, 1994: The effect of neglecting the virtual temperature correction on CAPE calculations. *Wea. Forecasting*, **9**, 625–629.
- Giorgi, F., 1991: Sensitivity of simulated summertime precipitation over the western United States to different physics parameterizations. *Mon. Wea. Rev.*, **119**, 2780–2888.
- Hart, R. E., G. S. Forbes, and R. H. Grumm, 1998: The use of hourly model-generated soundings to forecast mesoscale phenomena. Part I: Initial assessment in forecasting warm-season phenomena. *Wea. Forecasting*, **13**, 1165–1185.
- Janjić, Z. I., 1994: The step-mountain eta coordinate model: Further developments of the convection, viscous sublayer, and turbulence closure schemes. *Mon. Wea. Rev.*, **122**, 927–945.
- Kain, J. S., and J. M. Fritsch, 1992: The role of the convective “trigger function” in numerical forecasts of mesoscale convective systems. *Meteor. Atmos. Phys.*, **49**, 93–106.
- , and —, 1993: Convective parameterization for mesoscale models: The Kain–Fritsch scheme. *The Representation of Cumulus Convection in Numerical Models of the Atmosphere*, Meteor. Monogr., No. 46, Amer. Meteor. Soc., 165–170.
- , M. E. Baldwin, P. R. Janish, and S. J. Weiss, 2001: Utilizing the Eta Model with two different convective parameterizations to predict convective initiation and evolution at the SPC. Preprints, *Ninth Conf. on Mesoscale Processes*, Fort Lauderdale, FL, Amer. Meteor. Soc., 91–95.
- Lanicci, J. M., and T. T. Warner, 1991: A synoptic climatology of the elevated mixed-layer inversion over the southern Great Plains in spring. Part I: Structure, dynamics, and seasonal evolution. *Wea. Forecasting*, **6**, 198–213.
- Lilly, D. K., 1960: On the theory of disturbances in a conditionally unstable atmosphere. *Mon. Wea. Rev.*, **88**, 1–17.
- Manikin, G., M. Baldwin, W. Collins, J. Gerrity, D. Keyser, Y. Lin, K. Mitchell, and E. Rogers, 2000: Changes to the NCEP Meso Eta runs: Extended range, added input, added output, convective

- changes. NWS Tech. Procedures Bull. 465, NOAA/NWS, Washington, DC, 85 pp. [Available online at <http://www.nws.noaa.gov/om/tpb/465.htm> and from Office of Meteorology, National Weather Service, 1325 East-West Highway, Silver Spring, MD 20910.]
- Mesinger, F., 1996: Improvements in quantitative precipitation forecasts with the Eta regional model at the National Centers for Environmental Prediction: The 48-km upgrade. *Bull. Amer. Meteor. Soc.*, **77**, 2637–2650.
- Molinari, J., and M. Dudek, 1986: Implicit versus explicit convective heating in numerical weather prediction models. *Mon. Wea. Rev.*, **114**, 1822–1831.
- Rosenthal, S. L., 1979: The sensitivity of simulated hurricane development to cumulus parameterization details. *Mon. Wea. Rev.*, **107**, 193–197.
- Zhao, Q., T. L. Black, and M. E. Baldwin, 1997: Implementation of the cloud prediction scheme in the Eta Model at NCEP. *Wea. Forecasting*, **12**, 697–712.